Different approaches for the characterization of a fractured karst aquifer

CLAUDIA CHERUBINI, NICOLA PASTORE, VINCENZO FRANCANI
DICA Department - DIIAR Department
Technical University of Bari – Technical University of Milan
Via Orabona 4 70100 Bari – Piazza Leonardo da Vinci 32 20133 Milan
ITALY
claudia.cherubini@poliba.it vincenzo.francani@polimi.it

Abstract: - Karstic aquifers contain dissolution-generated cavities whose geometry is characterized by high variability; their cross-sections may range from uniform elliptical shapes, to high and narrow fissures, to irregular shapes partly filled with rock fragments and terra rossa deposits. In these conduits turbulent groundwater flow conditions may occur; in other cases no flow conditions may be due to the existence of lenses of terra rossa. In the examined site, located in the city of Bari, characterized by a fractured and karstic aquifer, an hydrogeological reconstruction of the heterogeneities is carried out, in order to simulate subterranean draining conditions that prove to be as near as possible to the real ones. Two different approaches are applied; the first one, aimed at only reconstructing the level of fracturation by means of geostatistical interpolation, and the second one, more complete, where multiple realizations are generated and conditioned to borehole data (RQD population), in order to obtain a three-dimensional distribution of fracture frequency, cavities and terra rossa lenses in the aquifer.

Key-Words: - heterogeneity, fractures, cavities, geostatistics, simulations

1 Introduction

In fractured and karstic aquifers groundwater flow takes place not only in the existent fracture network, but also in the karstic draining system that has developed according to the geomorphologic evolution and to the structural geologic asset. Therefore, the permeability of karstic aquifers consists of three overlapping categories: matrix permeability, fractures permeability and conduits permeability, resulting in a variation of hydraulic conductivity by many orders of magnitude on different size scales.

Previous studies carried out in the area of the ex Gasometer, aimed at reconstructing the level of heterogeneity, have conducted simulations applying distinct approaches: 1) the discrete fracture model (horizontal parallel set) [13]; 2) stochastic fracture zone continuum model, [3], [4]: in this approach the conditions of anisotropy of the medium are expressed by the hydraulic conductivities of the whole rock mass; 3) a more detailed reconstruction of the heterogeneity has been obtained considering the available stratigraphic data: by means of the RQD data it has been possible to take into account the fracturing degree of the medium for significant depths by means of geostatistic interpolation [5]; 4) Another approach in which multiple realizations are generated and conditioned to borehole data (RQD population) [7], in order to obtain a three-dimensional distribution of the level of fracturation. A more detailed reconstruction of the heterogeneity has been obtained by taking into account also the data sets of the karstic cavities and 'terra rossa' lenses, acquired by direct observation of the available borehole data.

2 Geological and hydrogeological features of the area

The area of ex Gasometer is located in the city centre of Bari, it extends for about 1.3 ha, is essentially flat, and has an elevation of 4m above sea level. This area lies in the coastal zone of the city of Bari, along the murgian adriatic margin of Apulia region, about 250 m far from the coastline. The stratigraphic sequence is characterized by a calcareous-dolomitic mesozoic bedrock on which marine carbonatic rocks and subordinately continental transgressive sediments have stratified. The calcareous- dolomitic rocks can be referred to the sedimentary series of the Murgian limestones, constituted by a succession of limestones, dolomitic limestones and dolomites, well stratified, characterized by a global thickness of thousands of

meters. This substrate that shows flat folds oriented WNW-ESE, constitutes the frame over which the most recent pleistocenic deposits have been deposited: this succession appears to be more or less intensely fractured and interested by phenomena of karstic dissolution. The karst phenomenon appears with the presence of forms of surficial modeling and hypogeum forms frequently filled by residual materials, derived by the dissolution of the same calcareous rocks: in different parts it is easy to find highly fractured and karstified levels with alternation of inclusions of residual soil ("terra rossa") at different levels. The calcareous dolomitic rocks are present in the subsoil at depths variable from about 3 to 13 m. The upper lithology of these late-quaternary deposits is constituted by sandy-calcarenitic deposits of about 7m of thickness, frequently weathered, with rare well cemented levels, and more frequently with intercalations of markedly sandy levels [9]. The basal part of the quaternary formation is frequently less cemented, weathered and altered. The most recent parts of the local stratigraphic sequence are represented by the recent alluvial deposits (Olocene) that can be found in residual strips above the calcarenites and the sands and, in higher thicknesses, at the bottom of the stream furrows ("Lama" Balice and Lamasinata). The alluvial deposits are formed by heterometric elements of different nature comprising silts, sands and cobblestones, derived by the desegregation of the substrate and the cover soils, with the further contribution of fine residual material ("terra rossa"). The study area is morphologically depressed and is known historically with the name of "Lake of Marisabella". Through this area the water coming from the erosion rills known as "lame", imposed on the preexisting fracturation lines is drained [18]. These linear incision, of tectonic-rain nature, are represented by "Lama Balice" and "Lamasinata", localized western to the study area, that are now hidden by the urban development.

3 Geostatistical elaboration of RQD

In order to implement the hydrogeological model of the site, data obtained from the campaigns of investigation have been utilized. In particular a geostatistical analysis of geomechanical data (RQD) coming from boreholes made in the area has been carried out. In order to obtain a study based on a considerable number of data, the geostatistical analysis has been carried out from – 8 m to – 15 m of depth from the ground level [5]. The variable RQD, characterized, for all boreholes, by high variability, appears as a discrete variable, that is to say it doesn't assume all values among a specified interval, but either 0 or values included in a range from 10 to 60. It is therefore possible to assimilate it to a binary variable. In order to treat this variable in such a way it is necessary to subdivide it into two classes: the first one has RQD = 0, that could be assimilated to porous medium, and the second one is characterized by a distribution variable from 10 to 60 [5]. The methodology of treating the RQD as a binary variable corresponds in geostatistical terms to the application of the Indicator Kriging (I_K). A value equal to 0 has been assigned to those points in which RQD<10 (that is to say the class having just the 0 value) and 1 to those values of RQD that are higher than or equal to 10. The Indicator in fact allows a better individuation and distinction of the zone in which the medium could be treated as fractured (I_K =0) from the zone in which it could be treated as (equivalent) porous (I_K =0). Once these zones are defined, for each depth the frequency of the fractures at each meter has been calculated, making use of the Priest and Hudson expression [18]:

$$RQD = 100e^{0.1\lambda}\left(0.1\lambda + 1\right) \quad (1)$$

Once the mean value m of the above mentioned distribution relating to each meter of depth is calculated, the thickness b of the fractures at that depth will be equal to 1/m [5].

3.1 Hydrogeological model

On the basis of the analyses carried out in the two campaigns of investigations, it has been possible to effectuate a reconstruction of the soil top elevation: it has values variable from +4 m to +3 m above sea level. The hydrogeological model, coherently with the stratigraphical data, is made up of a superficial layer of porous material locally constituted by clay mixed with calcarenite, that crops out on the ground level and has got a thickness of about 8 m. The presence of limestone has been modeled by inserting, starting from -8m until -15m, for each meter, a number of layers equal to the mean value of the fracture distribution relating to the examined depth [5]. In each layer a fracture distribution has been assigned, that would follow the binary criterion of Indicator Kriging (I_K). In fact, once the Indicator Kriging has been performed, the above mentioned zoning operation has taken into account the values in the interpolated maps. At each meter of depth there will be therefore a different distribution (Figure 1 a, b, c) and also a different thickness of the fractures, that could be obtained from the fracture frequency per meter. Once assigned the value of fractures thickness to the model, at each meter, it is necessary

to calculate the hydraulic aperture a [2]. For laminar fluid flow through parallel joint walls, the equivalent cubic law aperture (a) [2] is defined by:

$$a = \left[\frac{12q\mu}{b(dp/dx)} \right]^{1/3} \quad (2)$$

Where: q = steady - state flow rate; b = width of the fracture; dp/dx = pressure gradient; μ = dynamic viscosity of the fluid. In the case study the calculated gradient is equal to 0.001. The same formula has been applied for the calculation of the hydraulic aperture of the vertical fractures, supposed having a distance of some meters from each other, with a thickness equal to 0.003 m [5]. On the basis of the available stratigraphical data, a reconstruction of the karstic cavities asset at each meter of depth, has been made by means of Ordinary Kriging. In fact it emerges from the stratigraphies that at each point the cavities having relevant thickness are placed just at one specified depth, and this depth is almost always different for each point. From the results of the interpolation (Fig.1c) it appears that the cavities are intercommunicant, therefore there are preferential pathways of subterranean draining that are directed to the sea. In particular, from the analysis of the map, it emerges that the depths at which cavities are found are increasing from the left to the right side of the model.

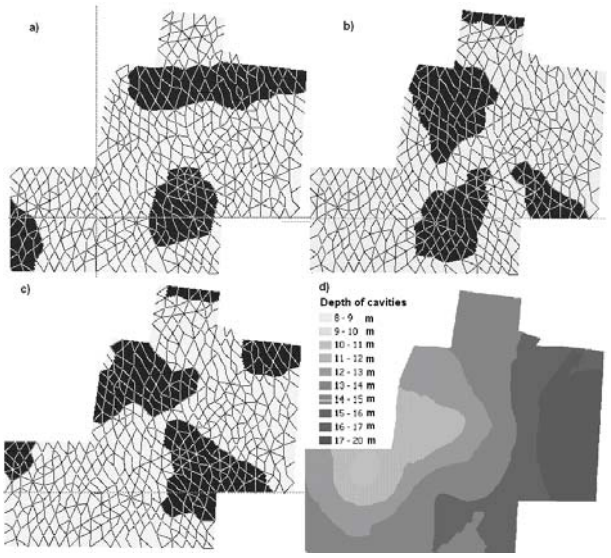

Fig.1 Distribution of fractures at -10 m (a), -12 m (b) and -15 m (c); distribution of karstic cavities with depth (d).

4 Second approach: RQD data analysis

In this approach from the punctual RQD index data, measured for each meter of depth, the joints distribution per cubic meter in the rock matrix blocks has been calculated, making use of the Palmstrom [15] expression:

$$RQD = 115 - 3.3 \cdot J_v \ (J_v = \text{Joints/m}^3) \quad (3)$$

The histogram of the distribution of Joints seems to belong to a bimodal distribution. A Multimodal distribution is a linear combination of two unimodal ones. The data set is divided into two parts, with proportional factors p_c and $(1-p_c)$. The resultant distribution is a linear combination of two normal distributions. The Gauss-Newton method is used to fit the empiric distribution by means of nonlinear least-squares in order to obtain the coefficients $(p, \mu_1, \sigma_1, \mu_2, \sigma_2)$. The Figg. 2-3 show the empirical and theoretical cumulative and density distribution of the joints.

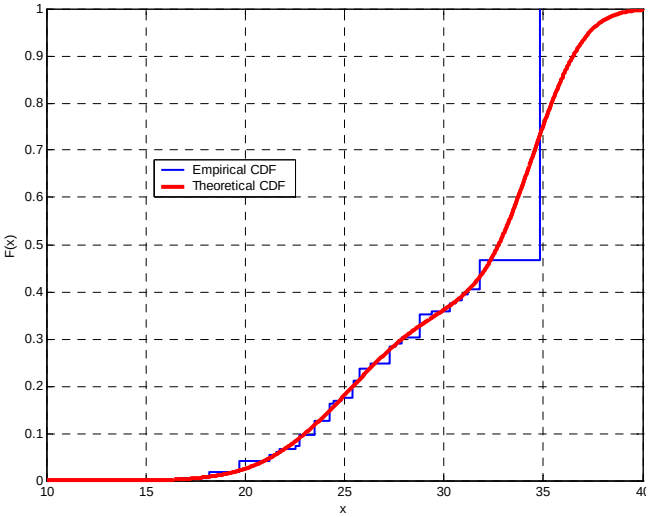

Fig.2 Empirical and theoretical cumulative distribution of the joints/m^3.

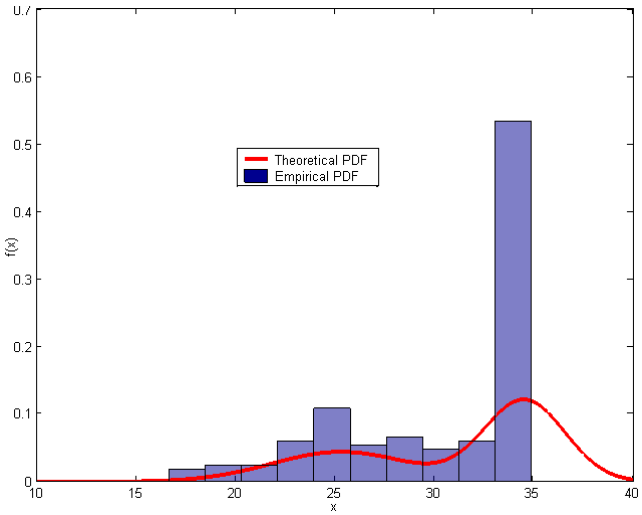

Fig.3 Empirical and theoretical density distribution of the joints/m^3.

4.1 Karstic cavities versus 'terra rossa' lenses

In this approach the data set of the karstic cavities and 'terra rossa' lenses, acquired by direct observation of the available borehole data, is treated as an indicator variable: to the 'terra rossa' lenses a value equal to '0' has been assigned, whereas to karstic cavities a value equal to '1'. Equally to the RQD index statistical analysis, the Histogram of distribution of this variable seems to belong to a bimodal distribution. The Figg.4-5 show the empirical and theoretical cumulative and density distribution of karstic cavities versus 'terra rossa' lenses.

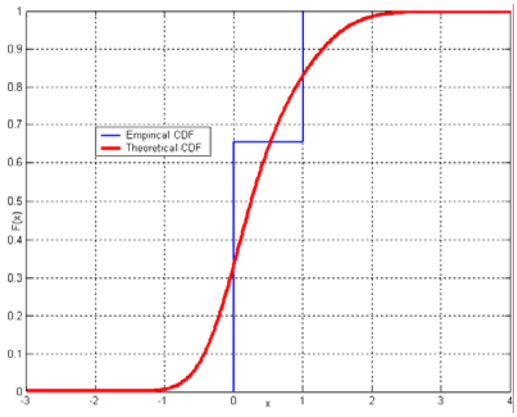

Fig.4 Empirical and theoretical cumulative distribution of the karstic cavities versus 'terra rossa' lenses.

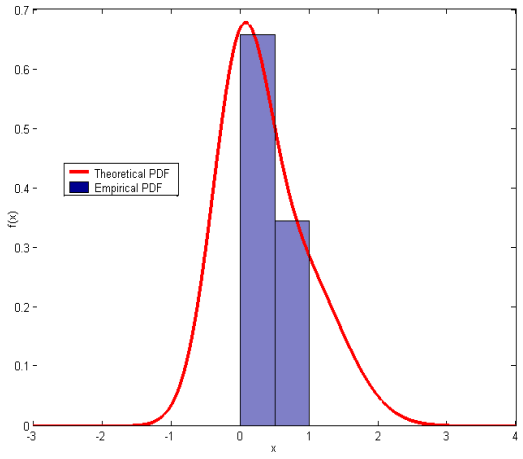

Fig.5 Empirical and theoretical density distribution of the karstic cavities and 'terra rossa' lenses.

The theoretical distribution of the joints and the cavities versus 'terra rossa' lenses are converted into a standard normal distribution by means of Gaussian anamorphosis [21]. This is a mathematical function which transforms a variable Y with any distribution into a new variable with a Gaussian distribution and vice versa. The Gaussian anamorphosis can be achieved using an expansion into Hermite polynomials $H_i(Y)$ [21]. The transformed data are used for stochastic simulation via stationary random field generation interpolation and then back-transformed to the original variables.

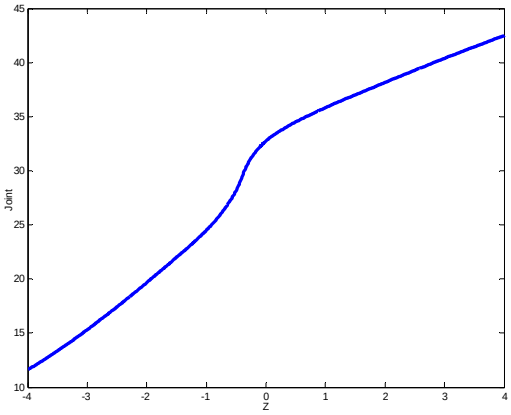

Fig.6 Gaussian anamorphosis for the joint/m^3 distribution.

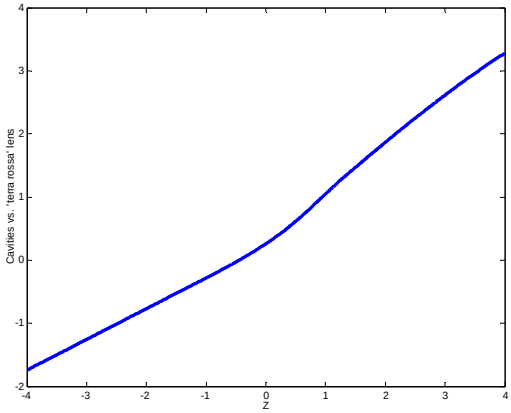

Fig.7 Gaussian anamorphosis for the cavities and 'terra rossa' lenses distribution.

4.2 Spatial analysis

In this study experimental variograms were not directly utilised, but were fitted by theoretical models. The fitting process is usually erroneous and biased, depending on the experimental variogram distribution and the geological knowledge. However in this work theoretical exponential variogram models with short and long-range structures present in the empirical variogram are used; they are obtained through weighted least square fitting process making use of the McBratney and Webster [11] weight expression:

$$w(h) = M(h) \cdot \hat{\gamma}(h) / E[\gamma(h)]^3 \quad (4)$$

The Geostatistical Software Library [8] and Simulated Annealing algorithm are used for the estimation of variogram model parameters. The theoretical variogram model for each variable is

converted into a covariance function (Figg.8-9) which is used for the generation of various independent stochastic simulations of the joints distribution and karstic cavities versus 'terra rossa' lenses distribution using Finite Fourier Transform properties. This method produces zero-mean stationary random field by inverse Fourier transforming independent random Fourier increments generated on a multi-dimensional wave number grid [1].

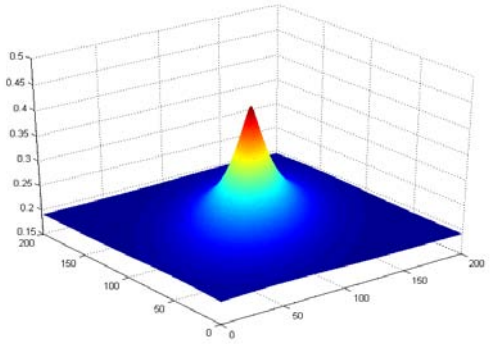

Fig.8 Covariance function of joint/m^3

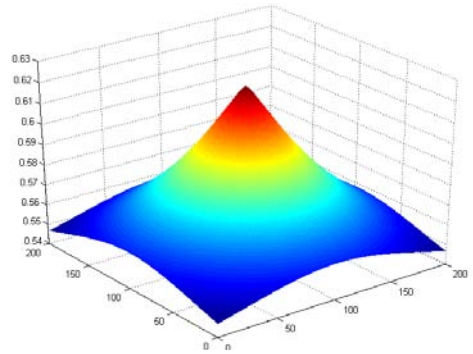

Fig.9 Covariance function of cavities vs. 'terra rossa' lenses.

The covariance matrix function is converted into the spectral density matrix using Finite Fourier Transform method:

$$s_k = \sum_{j=1}^{N} r_j e^{\frac{-2\pi i}{N}(j-1)(k-1)} \quad k = 1,...,N \tag{5}$$

Where N is the volume of the grid element.

The random Fourier increment can be constructed using the following expression:

$$y_k = s_k^{1/2} e^{i\theta(k)} N^{1/2} \quad k = 1,...,N \tag{6}$$

Where $\theta(k)$ is a phase angle random process uniformly distribuited in the range $[-\pi,+\pi]$.

The random field is obtained from the real part of the inverse finite fourier transform on the random Fourier increment:

$$Y_k^s = \left[\frac{1}{N} \sum_{j=1}^{N} y_k e^{\frac{2\pi i}{N}(j-1)(k-1)} \right]^{\mathrm{R}} \quad k = 1,...,N \tag{7}$$

Where R subscript indicates the real part.

Due to its random characteristic, a stochastic simulation process can output an infinite number of possibilities. Therefore the non conditional realizations are conditioned to the experimental hard data through a kriging step [10]:

$$Y_k^{cs} = Y_k^* + \left(Y_k^s - Y_k^{s*}\right) \tag{8}$$

Where Y_k^* and Y_k^{s*} is the simple kriging of the hard data values and the simulated values at the data locations.

Furthermore the soft data are used for the choice of the most plausible realization of the variables through the least square method. Finally these realizations are back-transformed into the original variables.

In Figg.10-11-12 are reported respectively, the distribution of karstic cavities, terra rossa lenses and joints at -10, -12, -13 and -15m.

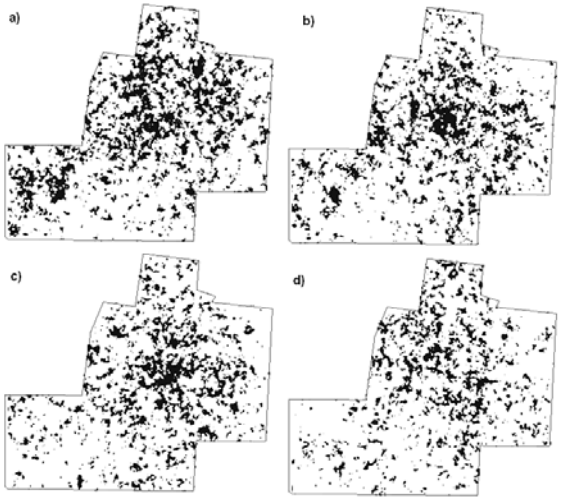

Fig.10 Distribution of karstic cavities at (a) -10, (b) -12, (c) -13 and (d) -15 m.

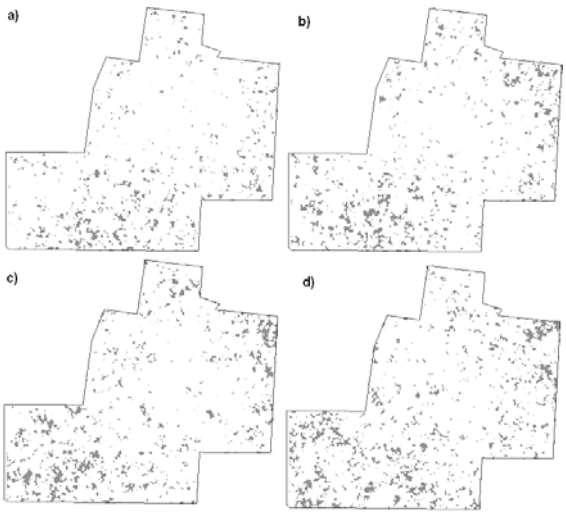

Fig.11 Distribution of terra rossa lenses at (a)-10 , (b) -12, (c) -13 and (d) -15 m.

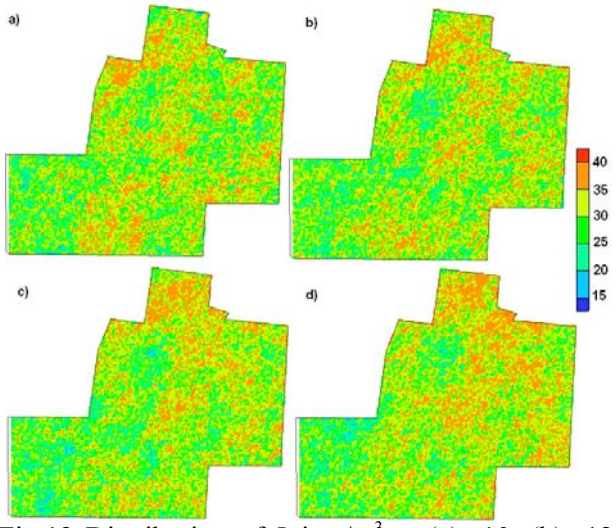

Fig.12 Distribution of Joints/m^3 at (a) -10, (b) -12, (c) -13 and (d) -15 m.

CONCLUSIONS

Modeling groundwater flow and contaminants propagation in fractured and karstic aquifers is affected by uncertainties caused by the high level of fracturation, by the presence of cavities that permit rapid groundwater propagation often in turbulent flow conditions and also by residual products that represent the immobile zone for the transport processes.

As a consequence, for modeling flow and transport in these aquifers it is not only necessary to define the level of fracturation, but also the conduits geometry and the immobile zone must be characterized. This allows to represent the mismatch of some orders of magnitude between high flow velocities within the karst conduits and lower

velocities in the fractured system and also the interaction between advective transport in mobile zones (fractures and karstic conduits) and storage of the contaminants in immobile zones. The proposed methodology in the study concerning the area of the ex Gasometer has allowed to build spatial models, at different degrees of detail, of the solution features [6] and anisotropy present in the aquifer, aimed at characterizing groundwater flow in fractured and karstic aquifers.

In the first approach, the piezometric heads derived from the flow simulation show, at each depth, a trend in the direction of downflow, going from SW to NE [5]. The obtained results are coherent also with the map of hydraulic conductivities [5], being the flow channeled up to the zones at higher values of conductivity, that is to say the ones characterized by a higher degree of fissuration and karstic erosion.

The carried out elaborations give just a schematical overview of the depth at which the most significant cavities can be detected.

The second approach permits to obtain a much more realistic impression of the heterogeneity of the phenomenon of interest, particularly it characterizes in a more detailed way the distribution of cavities at each investigated depth; moreover it takes also into account the distribution of 'terra rossa'.

The reconstruction of the distribution of cavities obtained by means of the second approach appears adherent with the hydraulic heads measured in situ. Previous studies [3], [4] show that the velocity fields obtained by means of an EPM approach proved to be not congruent with the ones measured in situ. This may affect the reliability of the estimation of contaminants propagation.

Contaminant transport in karstic aquifers is influenced by the dualistic nature of the flow system defined above. Even if the contaminants are rapidly transported in the conduit system, the effective contaminant propagation in the whole fractured system is much slower. Contaminant transport in fractured aquifers is affected by several processes among which advective transport, hydrodynamic dispersion, matrix diffusion and sorption. In fractured and karstic aquifers the dissolution cavities may contain abundant material especially colloidal–sized particles (<2μm) such as clays, organic matter, iron and alluminium oxides and hydroxides able to sorb chemicals from water. Due to the presence of these processes, karstic aquifers are highly vulnerable to groundwater contamination.

Although able to reconstruct similar hydrodynamic behaviors, the two proposed approaches may simulate different scenarios as far as contaminant transport is concerned.

In the first model, the solute transport is conditioned only by the level of fracturation and the presence of karstic cavities. In the second model, the presence of terra rossa inside the cavities may create further retardation in the migration of contaminants by removing solute (contaminant mass) from fracture flow by means of sorptive and diffusive phenomena.

To the contrary, remediation effectiveness in fractures is likely to be limited by reverse diffusion and desorption from the matrix [17]. For this reason, the application of the second approach in the implementation of a transport model may permit to simulate a more realistic scenario of contamination in order to plan effective remediation interventions.

References:

[1] Borgman L., Taheri, M. & Hagan, R., Three dimensional frequency domain simulations for geological variables. *Geostatistics for Natural Resources Characterization*, Part I, eds DG. Verly et al. Kluwer Academic M.A., 1984 pp.517,541.

[2] Indraratna B. and Ranjith P., *Hydromechanical aspects and unsaturated flow in jointed rock* A.A Balkema publishers, 2001.

[3] Cherubini Claudia, Giasi C.I., Masciopinto C. :Stochastic fracture flow modelling and influence of the computational procedures on the pollutants migration in a case study, *FEM MODFLOW Iternational Conference on Finite Element* . Karlovy Vary, Czech Republic, 2004.

[4] Cherubini Claudia, Giasi Concetta I., Flow and transport modelling and efficiency of remediation in a fractured and karstic aquifer: a case study, *IAHR-GW2006 "Groundwater in Complex Environments"* Toulouse, France 12-13-14 June 2006.

[5] Cherubini Claudia & Francani Vincenzo, A hydrodynamic model of a contaminated fractured aquifer, *Heat Transfer, Thermal Engineering and Environment.* Editors: S. Sorab, H. Katrakis. N. Kobasko, 2007.

[6] Cherubini Claudia, Giasi C.I, Pastore N., An efficient random field generator for the implementation of a hydrodynamic model of a contaminated fractured aquifer, *GQ07: Securing Groundwater Quality in Urban and Industrial Environments,* Fremantle, Western Australia, 2–7 December 2007.

[7] Dershowitz William S., La Pointe P. R., Doe Thomas W., Advances in Discrete Fracture Network Modeling: Current Status and Futere Trends *U.S. EPA/NGWA Fractured Rock Conference: State of the Science and Measuring Succes in Remediation*, 2004.

[8] Deutsch, C.V. and Journel, A.G., *GSLIB- Geo-statistical Software Library and User' s Guide*. Oxford University Press, England, 1992 pp. 39-60.

[9] Giasi C.I., Sulle problematiche connesse alla prevenzione della influenza marina sulle falde acquifere in aree carsiche, *Geologia Appl. e Idrogeol*. Vol XVII, 1982.

[10] Journel, A.G., Huijbregts, C.J., *Mining Geostatistics*, Academic Press, London, 1978 600 pp.

[11] Gross, M.R. an Engelder, T., Strain Accommodated by Brittle Failure in Adjacent Units of the Monterey Formation, USA: Scale Effects and Evidence for Uniform Displacement Boundary Conditions *Journal of Structural Geology*, 17(9), 1995, pp. 1303-1318.

[12] Masciopinto, C., Particles transport in a single fracture under variable flow regimes, *Advances in Engineering Software*, 35, 5, 1999, pp. 327-337.

[13] McBratney, A. B. and Webster R., Chosing functions for semi-variogram of soil properties and fitting them to sampling estimates, *J. Soil Sci*. 37, 1986, pp. 617-39.

[14] Miller, N., Predicting Flow Characteristics of a Lixiviant in a Fractured Crystalline Rock Mass. *Report of Investigations 9457, Bureau of Mines*, 24, 1993.

[15] Neretnieks, I., A note on fracture flow mechanisms in the ground, *Water Resources Research*, 19, 1983, pp. 364- 370.

[16] Palmström A., The volumetric joint count. A useful and simple measure of the degree of jointing, *4th Congress of the International Association of Engineering Geologists*, New Delhi, India, 1982, pp. 221–228.

[17] Parker, B.L., Gillham, R.W. and Cherry, J.A., Diffusive Disappearance of Dense, Immiscible Phase Organic Liquids In Fractured Geologic Media., *Journal of Ground Water*, 32, 1994, pp. 805-820.

[18] Pieri, P., Geologia della città di Bari ", *Memorie della Società Geologica Italiana*, v.14, 1975, pp. 379-407.

[19] Priest, S.D. and Hudson, J.A., Discontinuity spacings in rock, *International Journal of Rock Mechanics, Mining Science and Geomechanics* 1976, pp. 135–47.

[20] Rives, T., Razack, M., Petit, J.P. and Rawnsley, K.D., Joint Spacing: Analogue and Numerical Simulation, *Journal of Structural Geology*, 14(8/9) 1992, pp.925-937.

[21] Wackernagel H., *Multivariate Geostatistics: an introduction with Applications*, Springer-Verlag, Berlin, 3rd ed., 2003, 388 pp.